J. exp. Biol. (1979), **80**, 299–315
With 15 figures
Printed in Great Britain

AN ANALYSIS OF THE SHAPE AND PROPAGATION OF WAVES ON THE FLAGELLUM OF *CRITHIDIA ONCOPELTI*

BY D. N. JOHNSTON, N. R. SILVESTER AND M. E. J. HOLWILL
Department of Physics, Queen Elizabeth College, London W8 7AH

(*Received* 29 *August* 1978)

SUMMARY

1. Ciné micrographs were taken of the flagellated protozoan *Crithidia oncopelti* under dark-ground illumination. Coordinates of images of the flagella were obtained from the ciné frames by back-projection and automatic data acquisition.

2. The flagellar waveforms of proximally directed waves were characterized using a Fourier-series method and compared by this means with a number of analytical curves. The shape of a wave remained constant as it was propagated and, of the curves suggested, a wave consisting of circular arcs connected by straight lines gave the best fit.

3. The variation of bend curvature as bends moved along the flagellum was also found, for both proximally and distally directed waves.

4. The wavelengths and speeds of proximally directed waves increased linearly with distance as they approached the base of the flagellum, while in distally directed bends the curvature remained constant but the velocity increased as bends moved away from the base.

5. Causes of the above behaviour are discussed and it is concluded from the variation of curvature with time for proximally directed flagellar waves that unbending must be an active process.

INTRODUCTION

Waves of bending are propagated along flagella as a result of the mechanochemical reactions which occur within the organelles. The currently favoured hypothesis of flagellar bending, based on the evidence of electron and optical microscopy (Satir, 1976; Summers & Gibbons, 1971, 1973), assumes that relative sliding occurs between the various axonemal microtubules. These microtubular interactions become apparent as changes in the shape of the flagellum, and a careful examination of the shapes of the wave should yield useful information about the relative positions of the microtubules during movement. An exact knowledge of the wave shapes, and their behaviour as a function of time and of position along the flagellum, may also provide evidence of use in the construction of mechanochemical models of the system.

In hydrodynamic analyses of flagellar propulsion it is often convenient to approximate the wave shape by a sine wave (e.g. Holwill, 1977), although it is recognized that this is not an accurate representation of the real shape. While this sinusoidal approximation leads to reasonably accurate predictions of swimming speeds in certain cases,

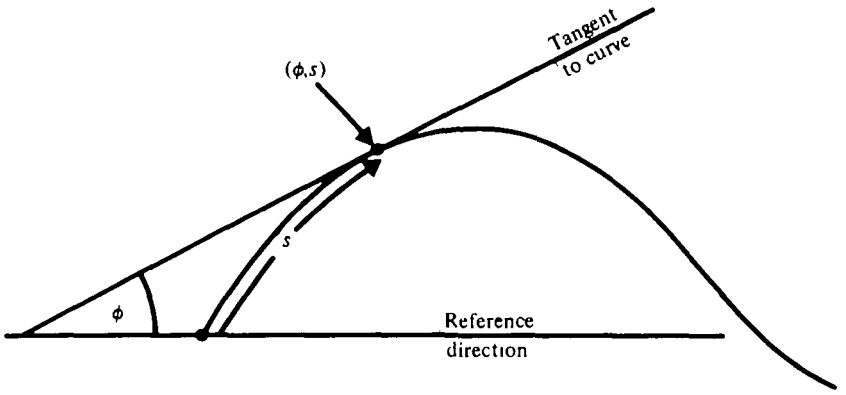

Fig. 1. Method of describing flagellar curve in terms of its tangent angle, ϕ, and arc length, s.

it cannot represent faithfully the re-entrant wave shapes which are often observed on flagella (Silvester & Holwill, 1972). Two alternative wave shapes which resemble flagellar waveforms, including re-entrant ones, more closely than a sinusoid have been analysed by Silvester & Holwill (1972). One is the waveform reported by Brokaw & Wright (1963) for *Ceratium* flagella, and consists of circular arcs linked by tangential straight lines – a shape which we shall refer to as arc-line. The other is the meander, the shape adopted by a river when flowing over relatively flat terrain. The same curve arises in the theory of random walks on a plane, and it also describes the bend which arises on a normally straight elastic beam when the two freely hinged ends are forced towards each other.

Silvester & Holwill (1972) showed that the meander, arc-line and sinusoidal waves could be distinguished from one another by representing the curves in terms of arc-length, s, and the angle $\phi(s)$ between the tangent to the curve at s and a fixed direction (Fig. 1). The sets of Fourier coefficients of the resulting graphs of ϕ versus s were readily distinguishable in the three cases. Experimentally, the parameters ϕ and s can be determined from photographs of flagella and comparisons can be made as described above between flagellar wave shapes and any of the theoretical curves. In this paper we report such a study of waves propagated by the flagellum of *Crithidia oncopelti* and we discuss the implications of the results.

THEORY

It is convenient to summarize here the mathematical properties of the three waves mentioned in the Introduction and to indicate how they may be distinguished analytically from each other. Quarter-wave sections of the three waveforms are shown in Fig. 2, where the x-direction lies along the axis of the wave. The curves are drawn such that λ_s/λ (where λ is the axial wavelength and λ_s the arc-wavelength) is the same for each. It is clear that in real (x, y) space the curves are similar and have no obvious distinguishing features. Distinct differences emerge if the curves of Fig. 2 are plotted in terms of $\phi(s)$ and s (Fig. 3). The curve corresponding to the arc-line shape shows a discontinuity, which occurs at the point of transition from circular arc to straight line. The gradient $d\phi/ds$ at any point of this curve is equal to the curvature

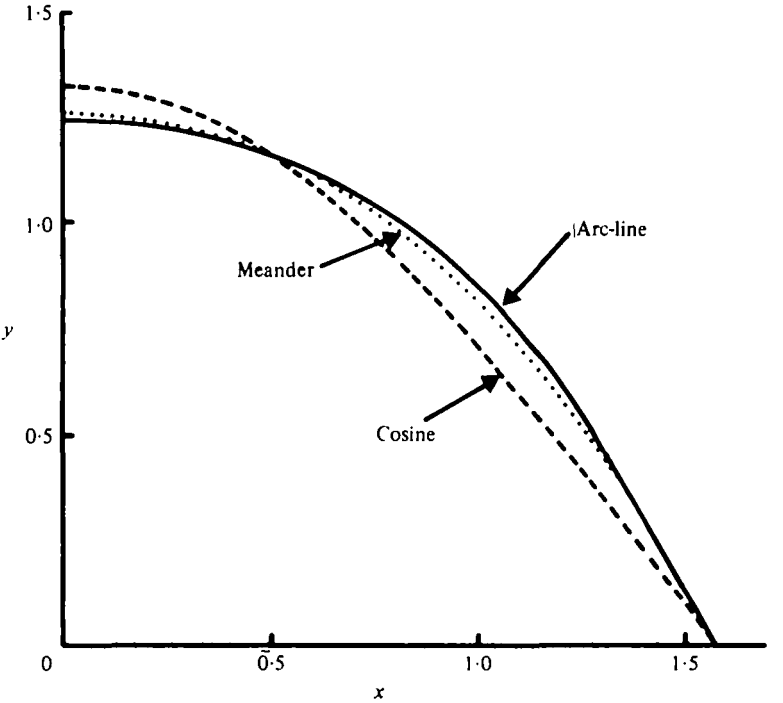

Fig. 2. Quarter-cycles of various waves possessing the same values of λ_s/λ.

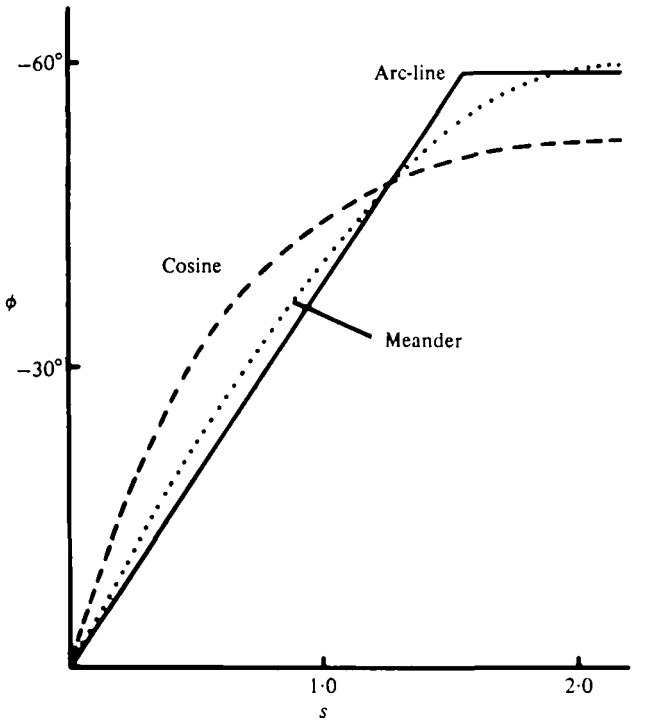

Fig. 3. Graphs of tangent angle, ϕ, versus arc length, s, corresponding to the three curves shown in Fig. 2.

Table 1. *Fourier coefficients b_1 to b_7 expressed as percentages (B_n) of b_1, for quarter-waves of various shapes*

Curve	Relative Fourier coefficients (% of b_1)						
	B_1	B_2	B_3	B_4	B_5	B_6	B_7
Sinusoid ($\lambda_s/\lambda = 1{\cdot}35$)	100	13·5	3·9	1·0	0·3	0	0
Arc-line							
(*a*) 92 % circular arc	100	−10·41	3·26	−1·31	0·53	−0·16	−0·04
(*b*) 76 % circular arc	100	− 5·09	1·33	1·92	−1·29	0·48	0·12
Meander ($\lambda_s/\lambda = 1{\cdot}35$)	100	0·3	0	0	0	0	0
Sine-generated wave	100	0	0	0	0	0	0
Tracked sine-generated controls							
(means from 12 quarter-waves)	100	− 0·04	0·19	0·20	−0·29	−0·02	−0·13
Standard deviations of above means	–	0·62	0·33	0·31	0·24	0·23	0·19
Tracked *C. oncopelti*							
(means from 259 quarter-waves)	100	− 5·03	1·63	−0·28	0·55	−0·06	0·13
Standard deviations of above means	–	0·57	0·26	0·21	0·16	0·17	0·10
Model sine-generated wave (see eqn. 3)*							
(*a*)	100	3·14	0·37	0·08	0·05	0·01	0·02
(*b*)	100	− 3·39	0·18	−0·01	0·02	0·01	−0·01

* (*a*) Leading quarter-waves, i.e. with zero curvature in advance of greatest curvature. (*b*) Trailing quarter-waves, with greatest curvature in advance of zero curvature.

of the real waveform at the same value of **s** and, in the case of the arc-line wave, is constant and finite for the circular section and zero in the straight region. The sine and meander curves are continuous when plotted as ϕ versus **s**, but the differences between them are more striking than in the y *v.* x plots of Fig. 2. It is relevant to note here that the meander is very similar to the 'sine-generated' wave for which $\phi \propto \sin \mathbf{s}$ (Langbein & Leopold, 1965). The $\phi(\mathbf{s})$ *v.* **s** curve for the meander is almost sinusoidal in form and cannot easily be distinguished from a curve corresponding to the sine-generated wave.

In order to compare the flagellar waveshapes with theoretical curves one could simply plot the experimental data in $\phi(\mathbf{s})$ *v.* **s** form and select visually that theoretical curve which appeared to fit the best. Such a technique is to some degree subjective, and assumes that the flagellar shape will be closely matched by one of the theoretical shapes which has already been postulated. It is therefore desirable to have a quantitative method which avoids any possible bias on the part of the observer and provides a succinct description of the flagellar shape for comparison with other theoretical curves which may be suggested in the future. A convenient way to achieve this is to represent the (ϕ, **s**) curve by a Fourier series of the form

$$\phi(\mathbf{s}) = \sum_n b_n \sin\left[(2n-1)\frac{\pi \mathbf{s}}{2S}\right], \tag{1}$$

where S is the length of the curve of the flagellar waveform to be analysed. The values of b_n are coefficients which characterize the various harmonic components of the curve and are given by

$$b_n = \frac{2}{S}\int_0^S \phi(\mathbf{s}) \sin\left[(2n-1)\frac{\pi \mathbf{s}}{2S}\right] d\mathbf{s} \tag{2}$$

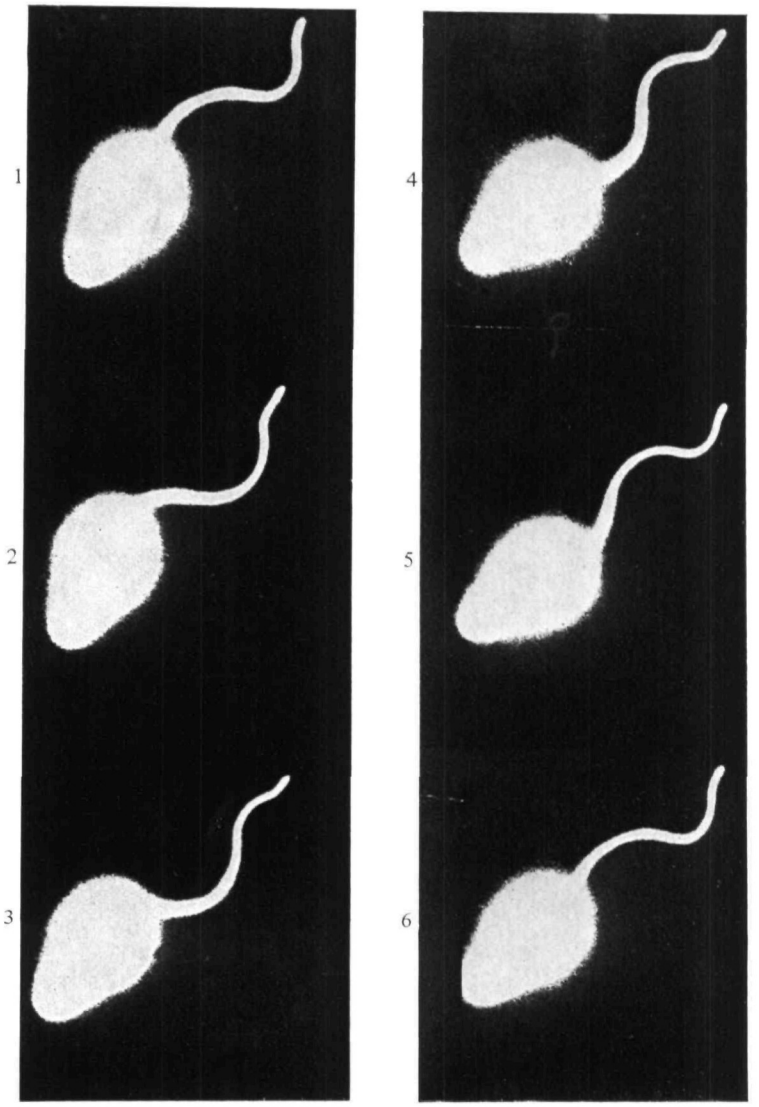

Fig. 4. A series of consecutive ciné frames of *Crithidia oncopelti* under dark-field illumination, showing motion of the flagellar wave from tip to base. The interval between frames is 10 ms.

A given curve has a unique set of values for the coefficients b_n (see, for example, Table 1 and Silvester & Holwill, 1972) so the flagellar wave shapes can be described unambiguously. Comparisons can then be made between the coefficients obtained from the image of a flagellum and the values of b_n obtained from theoretical curves, in particular those described above.

MATERIALS AND METHODS

A Zeiss RA research microscope fitted with a beam splitter to allow simultaneous viewing and filming of an object on the microscope stage was used to project images of *C. oncopelti* on to photographic film. Two light sources were used: one for viewing purposes, a xenon stroboscope (Chadwick Helmuth: Strobex model 99, Lamp 718) triggered by a variable-frequency oscillator and the other, for filming, a 300 W Super Pressure mercury lamp (Wotan, HBO). The former was used to align the microscope and for general viewing, since it had a minimal heating effect on the specimen. Just before filming, a mirror was rotated manually over the iris through which the light from the xenon lamp passed, so as to block this beam and reflect radiation from the mercury lamp into the condenser. The heating of the specimen by the mercury radiation was minimised by using it only for the duration of filming (one or two seconds). The microscope was used with a Zeiss dry, dark-field, condenser and a Zeiss 40× planapochromatic oil-immersion objective. A Zeiss FK 10× variable-focus eyepiece was used to focus images on the photographic emulsion of the ciné film.

Films were exposed in a Mitchell HS-16F4 ciné camera at a framing rate of 100 pictures/s (pps), giving an exposure time per frame of 2 ms. Kodak 4X (Type 7224) photographic film was used and was processed, after exposure, in a Gordon 16/35 continuous processor. Development was in Kodak DG-10 developer (diluted 1 to 6 with water) for 2 min at 20 °C. The film was then fixed in Kodak rapid fixer (diluted 1 to 3 with water) for 2 min. A typical series of high-contrast images obtained by this method is shown in Fig. 4.

Silvester & Johnston (1976) have described an automatic tracking device for the rapid recording of coordinates from flagellar images which have previously been filmed with dark-ground illumination. A photosensitive detector positioned over the back-projected image (final magnification × 3830) supplies signals to an analogue computer which alters the speed and direction of movement of the detector by controlling voltages fed to stepping motors. Cartesian coordinates are obtained in the form of voltages from linear potentiometers which are located along the x- and y-axes of the projected image and directly coupled to the position of the photosensitive cursor.

A digital computer (PDP-11/10s, Digital Equipment Corporation) was used to collect, store and display the Cartesian (x, y) coordinate pairs. A programmable unit (AR-11 interface) linked to the computer enabled analogue voltages from the two potentiometers to be sampled at a chosen rate (about twice a second) during automatic tracking. Each coordinate pair obtained in this way was displayed immediately on a Tektronix storage oscilloscope as a visual check against spurious data. The data were also punched on paper tape to give a record of the waveform for later analysis.

Sets of coordinates from different frames of ciné film were used as the input for a FORTRAN IV digital computer program which calculated values of ϕ, s and b_n (equations

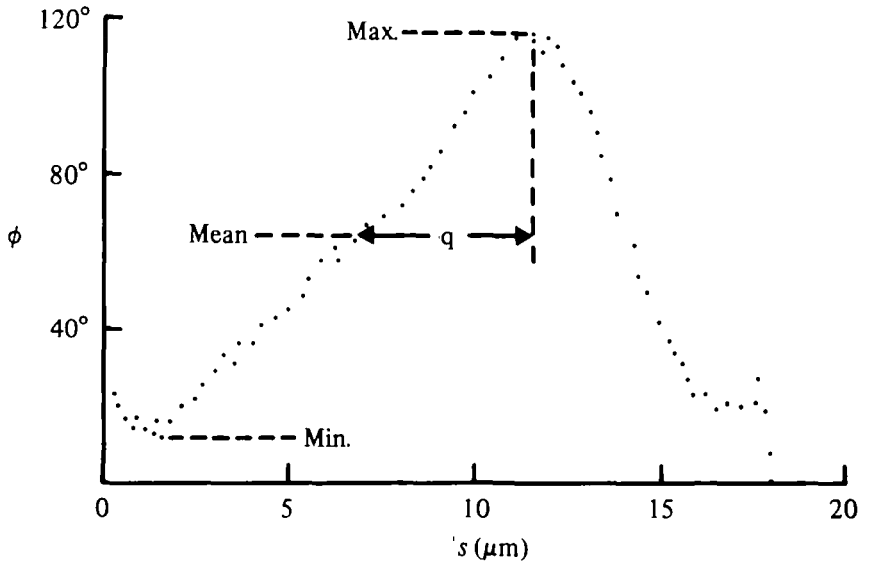

Fig. 5. Method of identifying quarter-wave sections (q) from (ϕ, s) data for harmonic analysis. The data shown here are from a typical flagellum but for clarity the number of points plotted in this figure is about a third of that recorded during tracking.

(1) and (2)). For convenience, output from the computer was recorded on microfilm (DIMFILM, University of London Computer Centre). In *Crithidia* it can be seen that the flagellar wave shape alters as an individual bend moves along the flagellum. To obtain a quantitative estimate of this change, and to overcome the analytical problems of working with a non-uniform flagellar wave train, the flagellum was divided into quarter-wave segments for analysis. From plots of ϕ versus s, half-wave segments were selected which lay between successive turning points of the curves (see Fig. 5). The corresponding set of data was divided into two groups, lying above and below the mean value of ϕ, thus defining two quarter-wave segments for analysis. The groups of data were manipulated to orient all the quarter-waves as shown in Fig. 3 and values of b_n were derived by using equation (2) and suitable iterative numerical integration procedures (Pennington, 1970; Johnston, 1978).

To test the accuracy of the experimental and numerical procedures, sine-generated curves which had approximately the same width, amplitude and wavelength as waves observed in ciné films of *Crithidia* flagella were produced on 16 mm microfilm. These 'control' images were tracked and the resulting data processed as described above to obtain values for the Fourier coefficients which were compared with analytically calculated values of b_n. Similar experiments were performed with slightly defocused control images, to simulate the indistinct edges in images of real flagella.

In total 77 frames of data collected from 16 individual organisms were examined with an average of about 140 coordinate pairs being recorded for each frame. A typical frame is reproduced in Fig. 6. Sections of waves taken from the tip or base often had lengths between 0 and 0·25 wavelengths and were not used in the final statistical calculations since their analysis as full quarter waves would have produced erroneous coefficients. The number of coordinate pairs used in each quarter-wave Fourier fit lay between 12 and 70 with a mean of about 30 points depending on the individual

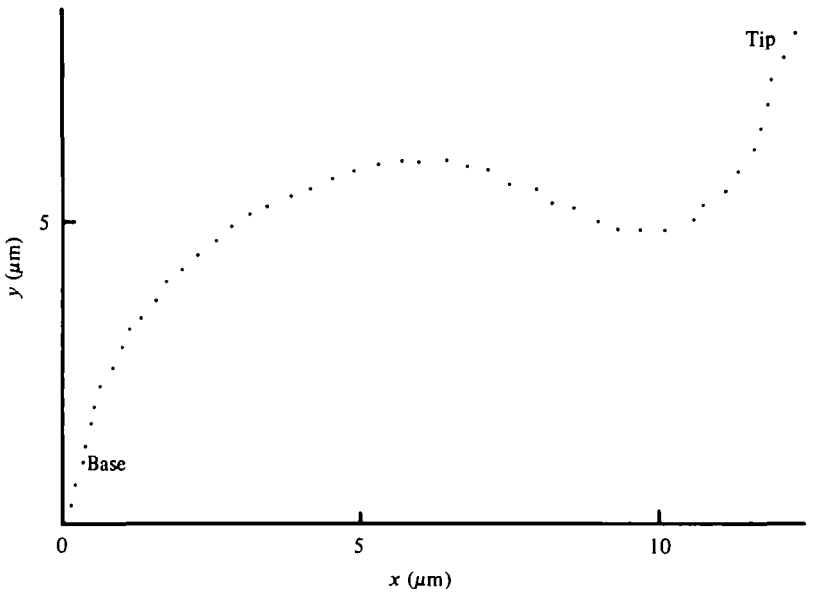

Fig. 6. The x, y data recorded during tracking of a ciné frame of *C. oncopelti*. (For clarity, only every fourth data point is plotted here.) The corresponding ϕ, s data are shown in Fig. 5.

flagellum. Each quarter wave was assigned a value of s corresponding to the position of its maximum curvature along the flagellum.

We also obtained values for the mean curvatures ($d\phi/ds$) from half-wave segments of the flagellum by measuring the mean slope of the approximately straight regions of the ϕ, s curves (Fig. 5). In this way we found how the curvatures of the bends varied as they moved along the flagellum. This was done both for normally beating flagella (waves propagated from tip to base) and for those in which waves travelled from base to tip.

RESULTS

By analysing sine-generated waves as a control and examining their Fourier coefficients it was possible to obtain estimates of the errors introduced by the experimental and numerical processes, since in this case only the first term in the Fourier expansion (b_1) should be present, all the higher terms having zero amplitude. Results of this test are presented in Table 1, where the relative amplitudes of the coefficients are presented as percentages (B_n) of the first coefficient. It can be seen that the experimentally derived value of B_2 is closer to zero than its own random error, which is 0·6 %, while the relative values of higher coefficients have random errors of about 0·3 % and also show no significant deviations from zero. Slight defocusing of the control images was found to have no adverse effect on the stability of the tracking process.

Values of B_n for quarter waves taken from *Crithidia* flagella were calculated and plotted against s for each coefficient. The resulting scatter-graphs for the second and third coefficients for all organisms examined are shown in Figs. 7 and 8. These plots reveal a variation in the relative amplitudes of the coefficients at different points along

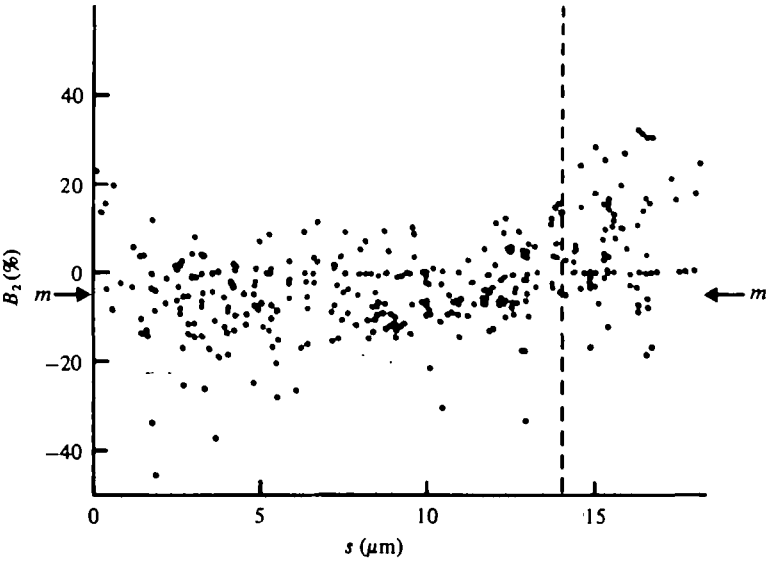

Fig. 7. Values of the second Fourier coefficient (b_2) as a percentage of the first, plotted against the position of the corresponding quarter-wave along the flagellar length. (m denotes the mean value for the points on the left of the dashed line.)

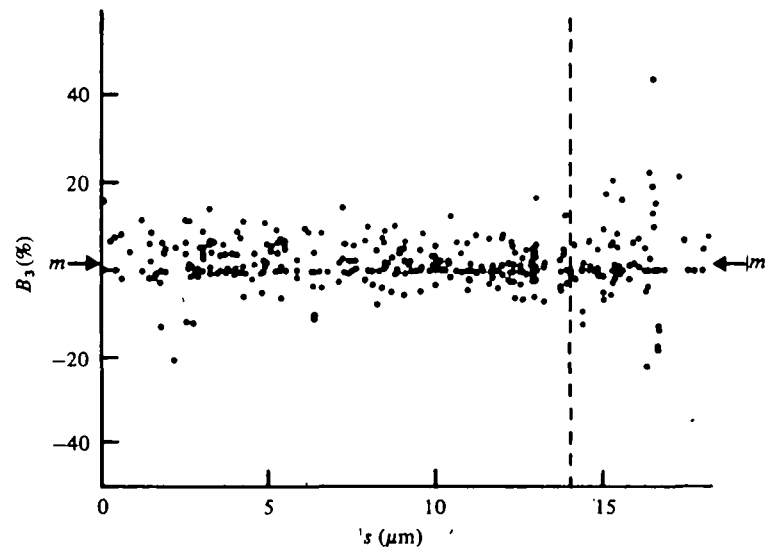

Fig. 8. Values of the third Fourier coefficient (b_3) as a percentage of the first, plotted against the position of the corresponding quarter-wave along the flagellar length. (m denotes the mean value for the points on the left of the dashed line.)

the flagellum. Over the approximate range $s = 0-14\ \mu m$ (indicated by the dashed lines in the figures) the spread of points remains roughly constant, while over the range $s = 14-18\ \mu m$ the spread increases. We used only the coefficients from the lower range ($s = 0-14\ \mu m$) and the mean values of B_n and their standard errors are shown in Table 1 (the means are indicated by the arrows in Figs. 7 and 8). For comparison the theoretical values of B_n for hypothetical shapes are also tabulated. A

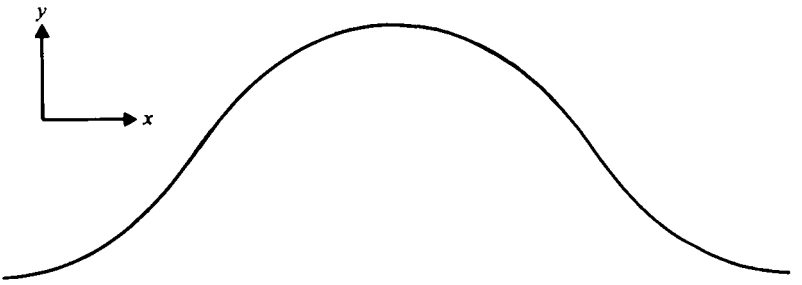

Fig. 9. A generalized wave shape for *Crithidia oncopelti*, reconstructed from the mean experimental values of B_n obtained by the analysis of about 200 quarter-waves.

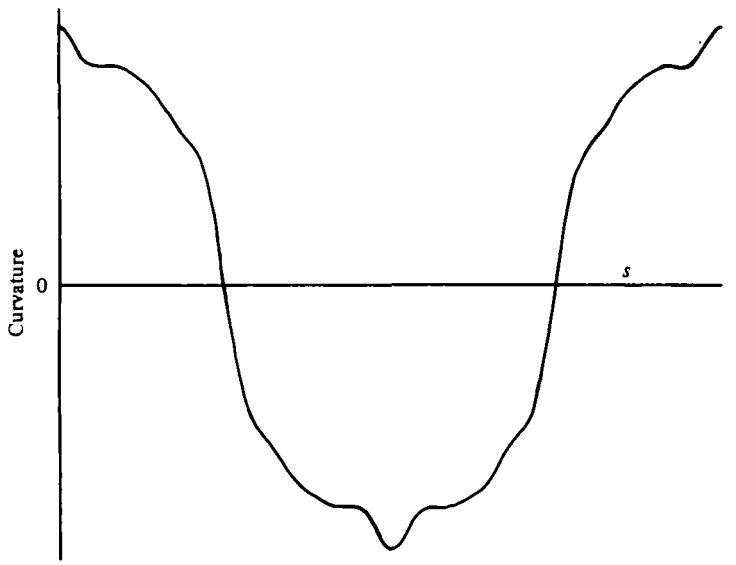

Fig. 10. Curvature plotted against arc length for the generalized wave shape shown in the previous figure.

generalized wave shape for *Crithidia*, reconstructed from the mean experimental values of B_n, is shown in Fig. 9. The corresponding graph of curvature against s for this wave shape is shown in Fig. 10.

We have also attempted to describe the observed ϕ, s curves for a *whole* flagellum, in terms of a sine-generated wave which moves from the tip of the flagellum to the base with a speed which increases linearly with distance from the distal end. This reflects the experimental observation that in *C. oncopelti* the wavelengths of the flagellar waves increase as they approach the base. In addition, the amplitude of the ϕ, s curve increases as it leaves the tip and this was simulated by making the ϕ amplitude of the sine-generated wave increase to a steady value in the manner of $(1-e^{-x})$. The resulting travelling wave which was fitted to the observed results was of the form shown below:

$$\phi = A(1-\exp(-mr))\sin 2\pi(k\log(1+r/s_0)-T), \tag{3}$$

where A is the maximum value of ϕ, r is a normalized distance along the flagellum which increases from 0 at the *tip* to 1 at the *base*, and k, s_0 and m are constants. T

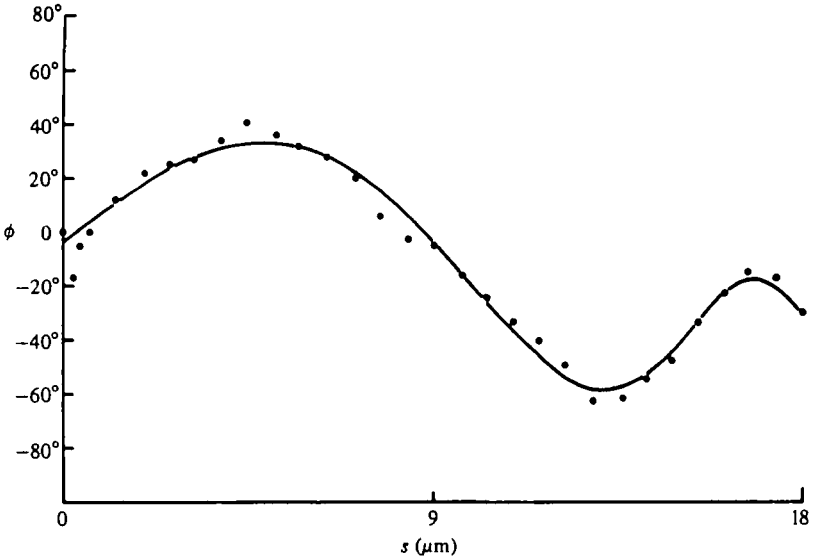

Fig. 11. The result of fitting equation (3) (see text) to ϕ, s values from the whole length of a typical flagellum. The theoretical curve is represented by the solid line and the experimental values by the points.

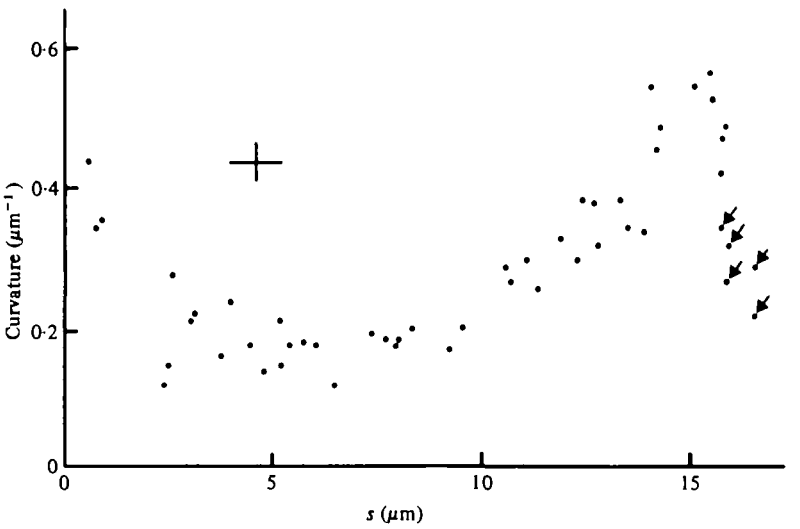

Fig. 12. Curvature data from 20 ciné frames of an individual flagellum corresponding to about five flagellar-beat periods. The arrowed points are probably atypical (see text). The cross represents an estimate of the error associated with each point.

represents time measured in units of the flagellar beat period. The speed of the travelling wave can be shown to be $dr/dT = (r+s_0)/k$, i.e. a speed which increases linearly with r, the normalized distance from the tip. (The logarithm in the above equation is thus necessary to describe the observed variation in speed and wavelength.)

Typical values obtained on fitting the parameters to the data from selected ciné frames of flagella were: $A = 60°$, $k = 0{\cdot}65$, $s = 0{\cdot}17$, $m = 15$. The root-mean-square deviation of predicted values of ϕ from the real data points was typically 8–13° and the

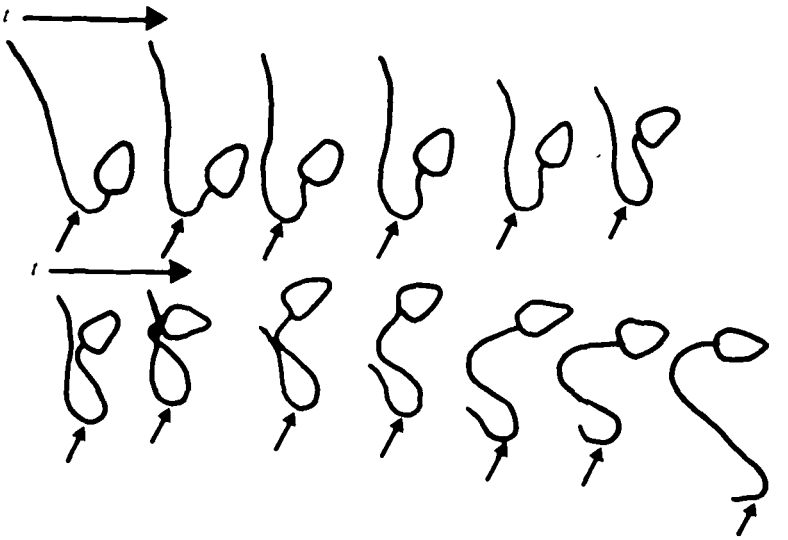

Fig. 13. Tracings from consecutive ciné frames of *C. oncopelti* beating in reverse and propagating an asymmetrical bend (arrowed) from base to tip. The interval between frames is 10 ms. Time (t) increases from left to right and the lower sequence follows directly on the upper one.

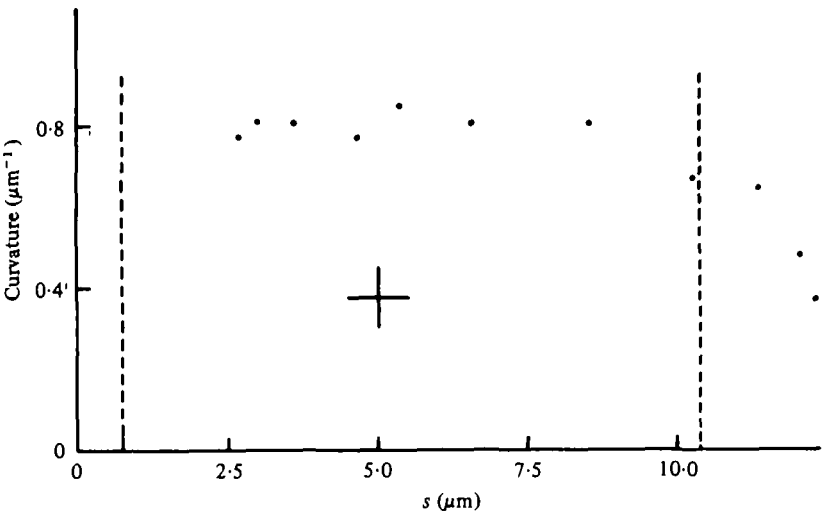

Fig. 14. Curvature data for a single flagellar bend moving from base to tip. The measurements extend over one period of the flagellar beat. The dashed lines enclose observations which were made while both extremities of the bend were visible on the flagellum. The cross represents an estimate of the error associated with each point.

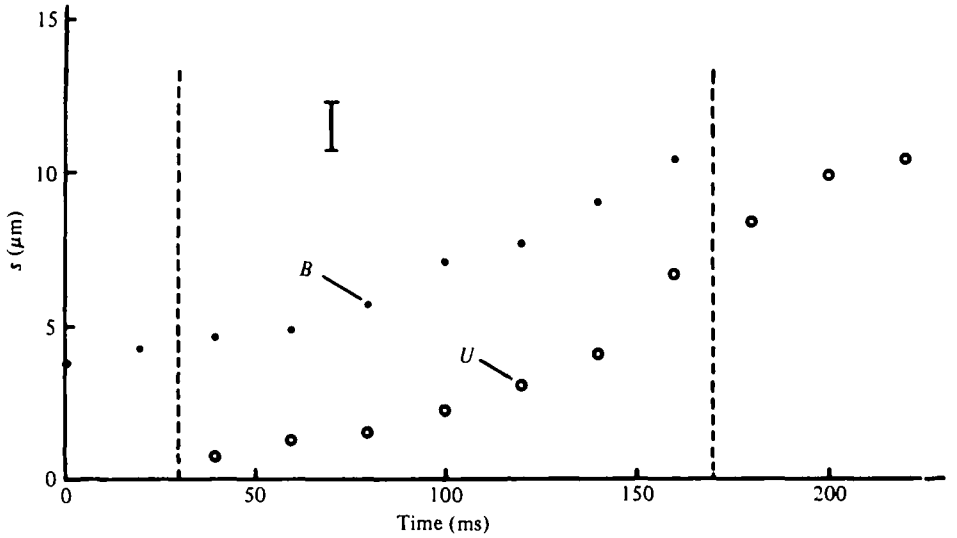

Fig. 15. The positions of the bending points (closed circles) and unbending points (open circles) of the bend described by the previous figure, plotted as a function of time. The dashed lines enclose the time during which both bending and unbending points were visible. The vertical bar represents the error in determining the positions of the bending points.

fitted curves seemed to give a satisfactory visual match with the ϕ, s curves (Fig. 11). However, to obtain quantitative comparisons with the experimental data, wave segments of this model travelling sine-generated wave were analysed in terms of their Fourier coefficients, and the resulting values are shown in Table 1.

The Fourier coefficients for two other wave shapes were also calculated for comparison with the experimental results. One of these was a series of meander arcs joined by straight regions while the other consisted of circular arcs linked by the 'straight' sections of a meander. The precise form of either curve can be adjusted by varying the proportion of the two shapes present on the wave, and this was done in an attempt to fit the experimental data. It was not possible to obtain a closer match to the set of experimental coefficients with either wave shape than has been obtained with the arc-line wave. The reasons for considering these particular wave shapes will be clarified in the Discussion.

Some typical results of analysing the curvature of the flagella are shown in Fig. 12, which displays data obtained from twenty frames of ciné film (about 5 flagellar beats) of one flagellum. Curvature is high at the tip and base of the organelle and has a minimum value between $s = 4\ \mu$m and $s = 7\ \mu$m. Some values (arrowed) may be considered as spurious since they were caused by a straight portion of the flagellum observed near the tip (see Discussion). These lower values were not obtained when data were collected from organelles showing no straight region at the tip.

On examining flagella which were propagating bends from base to tip, we found two forms of this reversed beating: at higher frequencies (*c.* 7 Hz) the waves appear symmetrical, whereas at lower frequencies (*c.* 3·5 Hz) they are asymmetrical The second form of beating is most commonly observed. Fig. 13 shows tracings from ciné frames of an organism propagating such an asymmetrical bend along its flagellum. It

can be seen that the curvature of the bend remains approximately constant until the bend approaches the tip of the organelle.

Fig. 14 shows typical values of curvature obtained from an organism beating in reverse as described above. The data are from a single bend which moved from base to tip. The curvatures are plotted against the distance the bend has travelled along the flagellum; the measurements extend over one period of the flagellar beat, i.e. about $\frac{1}{8}$ s. It can be seen that, over the region between the dotted lines, the curvature remained approximately constant. In Fig. 15 the closed and open circles show the positions of the 'bending' and 'unbending' points of the bend of the previous Figure, as a function of time. (These are defined visually (Brokaw, 1970) as the points of transition on the flagellum between bent regions and those unaffected by the presence of the bend.) The distance between these extremities of the bend at any time remained approximately constant ($4{\cdot}3 \pm 0{\cdot}5\ \mu$m) over the beat period while the wave velocity, which is given by the slope of these curves, increased from 25 to 93 μm s^{-1}. The dashed lines in Figs. 14 and 15 enclose the time within which both the bending and unbending points were observable on the flagellum.

DISCUSSION

In this paper we have presented results obtained from a critical analysis, based on the Fourier technique described by Silvester & Holwill (1972), of waveforms on the flagellum of the protozoan *Crithidia oncopelti*. Coordinate data from the waveforms were recorded using the system described by Silvester & Johnston (1976). The accuracy of the recording technique can be assessed by inspection of the coefficients for tracked sine-generated controls shown in Table 1. It can be seen that the experimental values agree with the theoretical ones (i.e. all zero exept B_1) within the limits of experimental error, indicating that the method is sufficiently accurate for analytical purposes.

The distribution of the coefficients, B_n, for flagella about their mean values is approximately symmetric within the range $0 \leqslant s \leqslant 14\ \mu$m (e.g. Figs. 7, 8) thus indicating that the type of wave form remains unaltered as a bend propagates, although the amplitude and wavelength may vary. The greater spread in the values of the coefficients, and the asymmetry, apparent for values of s larger than 14 μm, is due to the presence beyond this length of a straight section which requires coefficients of greater magnitude for its representation. Inspection of the mean values of the coefficients and their standard errors (Table 1) shows that the quarter-wave sections of the flagellum of *C. oncopelti* are more closely approximated by the arc-line wave than by the sine wave or meander. Since significant differences exist between the mean experimental values and those for sine waves or meanders, the probability that these shapes accurately represent flagellar wave shapes is small. The experimental values do not match exactly those of an arc-line wave with a particular ratio of circular arc length to straight line length, but fall in a region where there is between 76 and 92 % circular arc. These results are thus reasonably consistent with the view of Brokaw and others (e.g. Brokaw & Wright, 1963; Brokaw, 1965; Goldstein, 1977), which is that flagellar waves are basically arc-line in character, although the authors do not preclude the possibility that an alternative description is possible.

One alternative which we considered is represented by equation (3) (p. 307) and is based on the sine-generated approximation to a meander with modifications to allow for the increase in amplitude of ϕ and arc-wavelength which occur as a wave is propagated. The effect of the modifications is to cause the coefficients other than B_1 to be non-zero, as shown in Table 1. This variation of the coefficients is, however, different from that found experimentally and we conclude that the curve represented by equation (3), although it visually approximates the wave forms seen on *Crithidia*, does not provide an accurate description of flagellar wave shapes when judged by the criteria of Fourier-series analysis.

The mechanochemical events within a flagellum which give rise to bending, may also produce varying mechanical properties along the flagellar length. For example, the attachment of spokes to the central sheath in one region of the organelle (Warner & Satir, 1974) may impart to that region different elastic properties from those of a region where spokes are unattached. It is thus possible that bending in one section of the flagellum is dominated by its elastic properties whereas in a neighbouring region the elasticity of the system has a negligible effect on deformation. We therefore considered two further shapes for analysis: the first, meander curves linked by straight regions and the second, circular arcs linked by sections of a meander curve. Although each of these two wave forms can be generated in such a way as to give a reasonable visual match to the flagellar wave shape, in neither case does the set of Fourier coefficients approximate to the experimental set as well as the arc-line coefficients.

We are therefore led to conclude that the form of flagellar waves on *Crithidia oncopelti* is predominantly arc-line in character, with small deviations induced by the mechanism and structure of the system. Brokaw (1966) has suggested that the transition from circular arc to a straight line represents an abrupt change in terms of molecular mechanisms. If this hypothesis is correct, as Brokaw notes, the elastic elements which the flagellar system undoubtedly contains, together with the fluid viscosity, will cause the curvature at the transition points to change smoothly rather than discontinuously, even if the active internal forces exhibit discontinuous behaviour.

The available evidence suggests as a model for flagellar bending an active mechanism (the sliding microtubules) which tends to bend the flagellum into a circular arc, with the motion of the system influenced by elasticity and viscous interaction between the flagellum and its fluid environment. Since the velocity of a bend on the flagellum of *Crithidia* is approximately constant over a quarter wave, the data of curvature against s (Fig. 10) derived from the average wave shape of the flagellum also represent the variation of curvature with time over a quarter cycle and may therefore be used to examine the role of elasticity in the behaviour of the system. Now it can be shown theoretically that the curvature of an elastic rod subjected to an active bending moment and immersed in a viscous fluid will approach a maximum value (which will depend on the elastic properties of the rod) with a dependence upon time, t, of $(1-e^{-kt})$, where k is a constant. If the moment is suddenly reduced to zero with the rod in a bent configuration, the passive elastic forces within the rod will cause it to straighten in such a way that the curvature decays exponentially with time, as (e^{-kt}). Although the increases from zero of absolute curvature with time shown by Fig. 10 can be matched reasonably by a term of the form $(1-e^{-kt})$, the decreases of absolu

curvature towards zero do not exhibit exponential decay, so that unbending is not dominated by passive elasticity. We are led to conclude that unbending, as well as bending, is induced by active components within the flagellum. It is, however, not possible to obtain from our observations unequivocal information about the magnitude of the elastic constants characteristic of the flagellum. (A knowledge of these would enable more information about the time-dependence of the active bending moments to be deduced from the observed variation of curvature.)

The extensive analysis performed on the waves propagating from tip to base could not be carried out on bends propagating in the reverse direction because the asymmetry which was generally present precluded objective division of the flagellum into quarter-wave sections. The half-wave analysis which was used for the waves propagating from base to tip revealed that a bend did not change its curvature during propagation until it reached the final 2 μm of the flagellum (Fig. 14). This behaviour differs from that of waves propagated from tip to base, in which case the curvature decreases as a bend leaves the tip and then increases markedly as a bend approaches the flagellar base (Fig. 12). A further difference is that the constant curvature of the distally directed waves is generally larger than the maximum curvature attained by waves moving towards the base. The significance of these differences is not clear but is presumably associated with the mechanism which is responsible for causing the wave direction to reverse. Since the proximally directed waves are usually propagated at a higher frequency than those which are directed distally, the greater curvature achieved in the latter case could be the result of a constant bending moment acting for a longer period of time. An alternative explanation for the greater curvature might lie in the dependence on the sliding rate of the force generated by the microtubules. If, as in muscle, greater forces are generated as the rate of sliding decreases, the slower a flagellum beats the greater will be the bending moment developed by the microtubules. A maximum limit to the curvature is probably set by the structure of the flagellum, so that an increase in the bending moment will have no effect on the curvature once the maximum value is reached. The slower rate of microtubular sliding could affect the length of the flagellum which is bent after conditions appropriate to maximum curvature have been reached. There is some indication that this may be the situation for distally directed waves, for which re-entrant shapes are often observed (Fig. 13; Holwill, 1965). However, this type of behaviour is not observed for waves propagating from tip to base along flagella in a medium sufficiently viscous to produce the lower frequencies (and hence the lower microtubular sliding velocities) observed on the distally directed waves (Holwill, 1965). It seems likely, therefore, that the differences in behaviour for the waves propagating in the two directions are associated with the mechanism for wave reversal rather than being inherent in the bending mechanism itself.

The speeds of bending and unbending points for distally propagated bends increase with distance along the flagellum (Fig. 15). A similar result is obtained for the proximal portion of sea-urchin sperm tails (Brokaw, 1970; Goldstein, 1977) but in that case, at distances greater than about 10 μm from the base, the unbending and bending points then travel at constant speed. For the sea-urchin sperm tail, the behaviour of the propagation velocities in the proximal region is probably associated with the proximity of the basal structures or the requirements for wave initiation, or possibly

with both. On the basis of this comparative observation, it appears that the *Crithidia* flagellum is sufficiently short that most of its length is affected by similar constraints to those in sea-urchin sperm.

Analyses of wave shapes for echinoderm spermatozoa have been presented by Rikmenspoel (1978) and by Hiramoto & Baba (1978). These authors report that the curvature of starfish and sea-urchin sperm tails can be described by a sinusoidal function of time with a phase term which is dependent on distance along the flagellum. In all cases studied the phase term was approximately proportional to distance over the whole flagellum except for the basal 10–15 μm. Since the flagella are about 50 μm in length, the major portion of the flagellum appears to form a sine-generated wave. In the basal region, the phase term no longer changes in a linear way with distance, so that the wave form in this part of the flagellum is not sine-generated, but assumes some other shape. There is insufficient information available to allow an evaluation to be made of the wave shape near the base, but it is reasonable to suppose that the modification to the shape has its origins in the same factors which cause the change in the propagation velocities discussed earlier, namely the influence of basal structures or the requirements for bend initiation.

Visual curve-fitting procedures have led to descriptions of flagellar wave shapes as arc-line (e.g. Brokaw, 1965) meander-like (e.g. Brokaw, Goldstein & Miller, 1970; Rikmenspoel, 1971) and sine-generated (Sarashina, 1974; Rikmenspoel, 1978; Hiramoto & Baba, 1978). As emphasized earlier in this paper, differentiation between these wave forms on the basis of a visual technique may incorporate subjective bias, and it is necessary to use objective methods, such as that described here, to avoid this problem. It would be interesting to apply the Fourier technique to the flagella studied by other authors so that an independent quantitative assessment of wave shape might be obtained.

One of us (D.N.J.) is grateful to Queen Elizabeth College for the receipt of a post-graduate scholarship. This work was supported in part by grants from the Science Research Council and the Central Research Fund of the University of London.

REFERENCES

BROKAW, C. J. (1965). Non-sinusoidal bending waves of sperm flagella. *J. exp. Biol.* **43**, 155–169.

BROKAW, C. J. (1966). Bend propagation along flagella. *Nature, Lond.* **209**, 161–163.

BROKAW, C. J. (1970). Bending moments in free-swimming flagella. *J. exp. Biol.* **53**, 445–464.

BROKAW, C. J., GOLDSTEIN, S. F. & MILLER, R. L. (1970). Recent studies on the motility of spermatozoa from some marine invertebrates. In *Comparative Spermatology* (ed. B. Baccetti), pp. 475–486 New York: Academic Press.

BROKAW, C. J. & WRIGHT, L. (1963). Bending waves of the posterior flagellum of *Ceratium*. *Science, N.Y.* **142**, 1169–1170.

GOLDSTEIN, S. F. (1977). Assymetric waveforms in echinoderm sperm flagella. *J. exp. Biol.* **71**, 157–170.

HIRAMOTO, Y. & BABA, S. (1978). A quantitative analysis of flagella movement in echinoderm spermatozoa. *J. exp. Biol.* **76**, 85–104.

HOLWILL, M. E. J. (1965). The motion of *Strigomonas oncopelti*. *J. exp. Biol.* **42**, 125–137.

HOLWILL, M. E. J. (1977). Some biophysical aspects of ciliary and flagellar motility. *Adv. Microb. Physiol.* **16**, pp. 1–48.

JOHNSTON, D. N. (1978). Theoretical and experimental aspects of flagellar wave shape analysis and their application to the protozoan *Crithidia oncopelti*. Ph.D. thesis, University of London.

LANGBEIN, W. B. & LEOPOLD, L. B. (1965). River meanders – theory of minimum variance. *Geol. Surv Prof. Paper* 422-H. Washington: U.S. Government Printing Office.

PENNINGTON, R. H. (1970). *Introductory Computer Methods and Numerical Analysis*. London: Macmillan.
RIKMENSPOEL, R. (1971). Contractile mechanisms in flagella. *Biophys. J.* **11**, 446–463.
RIKMENSPOEL, R. (1978). Movement of sea urchin sperm flagella. *J. Cell Biol.* **76**, 310–322.
SARASHINA, T. (1974). Numerical analysis on wavy track of nematodes. *Rep. Hokkaido Prefect. Agric. Exp. Stn* **23**, 1–48.
SATIR, P. (1976). Production and arrest of ciliary motility. In *Contractile Systems in Non-Muscle Tissues* (ed. S. V. Perry *et al.*), pp. 263–273. Amsterdam: Elsevier–North-Holland.
SILVESTER, N. R. & HOLWILL, M. E. J. (1972). An analysis of hypothetical flagellar waveforms. *J. theor. Biol.* **35**, 505–523.
SILVESTER, N. R. & JOHNSON, D. N. (1976). An electro-optical curve follower with analogue control. *J. Phys.* (E: Sci. Instrum.) **9**, 990–995.
SUMMERS, K. E. & GIBBONS, I. R. (1971). ATP-induced sliding of tubules in trypsin-treated flagella of sea-urchin sperm. *Proc. natn. Acad. Sci. U.S.A.* **68**, 3092–3096.
SUMMERS, K. E. & GIBBONS, I. R. (1973). Effects of trypsin digestion on flagellar structures and their relationship to motility. *J. Cell Biol.* **58**, 618–629.
WARNER, F. D. & SATIR, P. (1974). The structural basis of ciliary bend formation. *J. Cell Biol.* **63**, 35–63.